Evaluation and Modeling of the Mechanical Behavior of Carbon Nanoparticle/Rubber-Modified Polyethylene Nanocomposites

Waleed E. Mahmoud, A. A. Al-Ghamdi, F. Al-Marzouki, S. Al-Ameer

Physics Department, Faculty of Science, King Abdulaziz University, Jeddah, Saudi Arabia

Received 7 December 2010; accepted 3 January 2011
DOI 10.1002/app.34107
Published online 6 July 2011 in Wiley Online Library (wileyonlinelibrary.com).

ABSTRACT: Recently, the production of polymers loaded with inorganic nanomaterials has been one of the most economical techniques playing a special role in improving the physical and mechanical properties of nanocomposites. Rubbers loaded with different concentrations of carbon nanoparticles (CNPs) were synthesized. The mechanical properties were tested according to standard methods. It was found that the properties of the investigated nanocomposites were improved, depending on the concentration of CNPs in the investigated composite. The optimum concentration was found to be 1.3 vol %. Affine deformation based on the Mooney–Rivilin model was used to visualize the effect of CNPs on the rubber. When polyethylene (PE) was added to rubber/CNPs at the optimum concentration (12.4 vol %), the modulus, tear resistance, and fatigue life were increased, whereas the tensile strength decreased, and the strain at rupture remained almost same. A crosslink model was used to explain the influence of PE on the rubber/CNP nanocomposites. © 2011 Wiley Periodicals, Inc. J Appl Polym Sci 122: 3023–3029, 2011

Key words: mechanical properties; nanocomposites; rubber

INTRODUCTION

In the field of conducting polymeric nanocomposites, one main objective is to minimize the filler concentration because a high concentration of the conductive filler could lead to the deterioration of the mechanical properties of the composite. Different conductive fillers, such as carbon black, graphite powder, and metallic powder, have been explored extensively for composite components, and usually, a higher filler content is loaded to achieve good electrical properties.

Fillers play important roles in modifying the desirable properties of polymers and reducing the cost of their composites. In conventional polymer composites, many inorganic filers with dimensions in the micrometer range, for example, calcium carbonate, glass beads, and talc, have been used extensively to enhance the mechanical properties of polymers. Such properties can indeed be tailored by changing the volume fraction, shape, and size of the filler particles.[1–3] A further improvement of the mechanical properties can be achieved through the use of filler materials with larger aspect ratios, such as short glass fibers.[4–6] The dispersion of fillers with dimensions in the nanometer level having very large aspect ratios and stiffnesses in a polymer matrix could lead to even higher mechanical performances.[7–10] These fillers include layered silicates and carbon nanotubes.[11,12] Rigid inorganic nanoparticles with smaller aspect ratio are also promising reinforcing and/or toughening materials for polymers. The dispersion of nanofillers in polymers is rather poor because of their incompatibility with polymers and large surface-to-volume ratio.[13,14] In this study, we aimed to examine the effect of polyethylene (PE) on the mechanical properties of carbon-nanoparticle (CNP)-loaded rubber composites to reduce the tendency of agglomeration of CNPs and to get rid of the poor dispersion of CNPs in the rubber matrix.

EXPERIMENTAL

A two-roll mill of length 0.3 m, radius 0.15 m, speed of slow roll 18 rpm, and gear ratio 1.4 was used to prepare such composites. During the mixing process, different ingredients were added as follows: 100 g of rubber was milled for 10 min, after which 2 g of stearic acid, used as coactivator, was added and mixed for 5 min. Zinc oxide (5 g), which used as an activator to enhance the action of organic accelerators, was added and mixed for 7 min. Different contents (0, 1, 2, 3, 4, and 5 g) of CNPs (purchased from Helix

Correspondence to: W. E. Mahmoud (w_e_mahmoud@yahoo.com).

Material Solution, Richardson, TX, 10-nm diameter), was added and mixed for 5 min. Dioctyle phthalate oil (10 g) was added and mixed for 4 min. Dibenzthiazyl disulfide (2 g) as an ultraaccelerator was added and mixed for 3 min. Phenyl-β-naphthyl amine (1 g) as an antioxidant was added and mixed for 3 min. Sulfar (2.5 g), which used as vulcanizing agent, was added and mixed for 5 min. The mixture was passed endwise 10 times through the mill at a 1-mm opening and after that was sheeted off at a 2-mm thickness. This process took about 8 min. The total milling time was fixed to about 50–55 min. The compounded rubber was left for at least 2 days before vulcanization. For nanocomposites modified with PE, different concentrations (5, 10, 15, and 20 g) of PE were mixed with the nanocomposite, which had 2 g of CNP by the same procedure.

The samples were compression-molded into sheets with a steel die, which had dimensions of 1×10^{-4} m^2 for area and 0.01 m for height. The vulcanization was conducted under a heating press (KARL KOLB, Germany) at a temperature (T) of 423 ± 2 K under a pressure (P) of 4 MPa for 30 min. The vulcanized samples were shelf-aged for 48 h at a temperature of 70°C in an electric oven before testing. The vulcanization conditions were fixed for all samples.

For mechanical measurements, the nanocomposites were in the form of strips 2 cm long, 2 mm wide, and 1 mm thick. The stress–strain behavior was measured at room temperature on the basis of ASTM D 412-8a standards with a material tester (AMETEK, USA), which was connected by a digital force gage (Hunter Spring ACCU Force II, 0.01-N resolutions) to measure the forces. The force gage interfaced with a computer to record the obtained data. The stress–strain behavior was measured at a strain rate of 0.01 mm/s. For electrical measurements, brass electrodes were attached to the parallel faces of the samples during vulcanization, and a digital electrometer (616 Keithly, Japan) was used. The dispersion of nanofiller and PE into the rubber matrix was visualized by field emission scanning electron microscopy, which was carried out with a JEOL 2010 (Japan) high-resolution transmission electron microscope at 200 kV.

RESULTS AND DISCUSSION

Percolation theory

The percolation threshold (V_c) is a basic characteristic of a conductive composite; in this case, V_c defined the composition range for studying the effect of CNP on conductivity. Figure 1 shows the variation of the resistivity with the volume fraction of filler (V). The model that is most often used to quantify the changes in the transition and conductive regions is the so-called statistical percolation model.[15] Proposed by Kirkpatrick[16] and Zallen,[17] this model predicts the electrical resistivity of an insulator–conductor binary mixture by assuming random positions of the filler particles. The result is a power-law variation of the resistivity (ρ) above V_c:

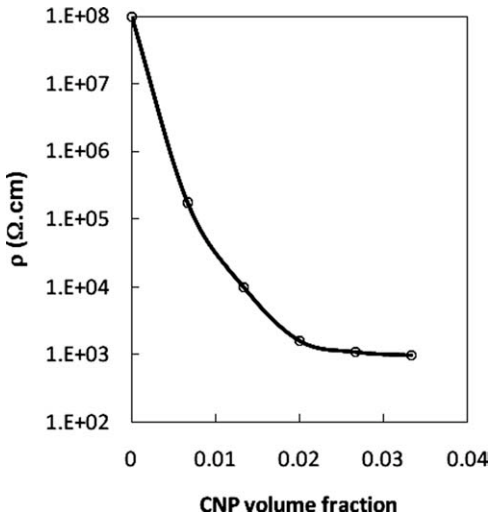

Figure 1 Resistivity versus the CNP volume fraction.

$$\rho \propto \left(\frac{V - V_c}{1 - V_c}\right)^{-t} \quad (1)$$

where t is a universal exponent. The two-parameter fit is represented in Figure 1 by the solid line and gives $V_c = 0.013$ and $t = 2.01$. The significant point here is that the percolation concentration was low compared with carbon black.[18] This may be attributed to the high aspect ratio of nanospherical particles.[19]

Mechanical properties

To initially visualize the effect of CNP loading on the mechanical characteristics of the rubber, Figure 2 depicts the stress–strain behavior up to failure of rubber loaded with different concentrations of CNPs (0, 0. 7, 1.3, 2, 2.6, and 3.5 vol %). It is clear that at a fixed strain, the stress increased monotonically as the amount of nanofiller increased. Compared with nitrile butadiene rubber (NBR)-loaded carbon black,[20–24] it is clear that very small amount of CNPs increased the hardness of the rubber by more than 5 orders more than carbon black filler, which required 50–60 vol % to obtain approximately the same improvement in hardness. To investigate the influence of CNP content on the mechanical properties of the rubber, the affine deformation based on the Mooney–Rivilin model was selected to visualize the mechanism of interaction of CNPs with rubber.

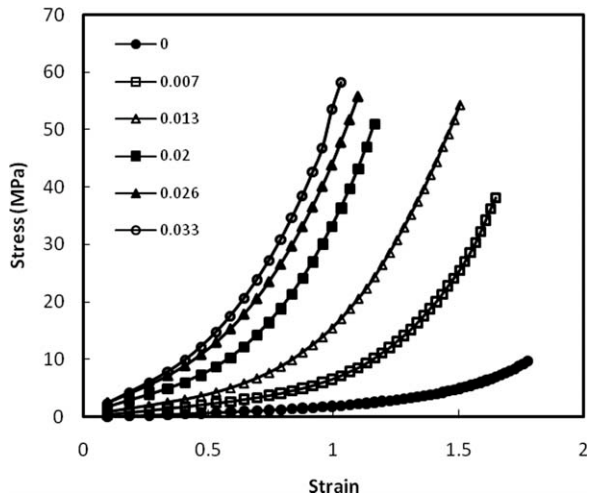

Figure 2 Stress–strain relationship for rubber loaded with different amounts of CNP.

The framework used to understand rubber elasticity at small deformations was established earlier by Treloar, Meyer, and Flory.[25] The affine deformation (components of vector length or end-to-end distance of each chain are changed in the same ratio as the corresponding dimensions of the bulk rubber) of a network of Gaussian chains can be equivalently understood from the perspective of thermodynamic elasticity[26] or strain invariants, such as storable elastic energy.[27] Starting from this foundation, the impact of various complexities, such as filler content, crosslink fluctuation, nonaffine deformation (phantom network theory[28]), distribution in crosslink functionality, chain constraints, and free chains, can be discussed. To establish a connection to these previous efforts and begin to quantitatively understand the unique impact of CNPs as fillers on rubbers, it is instructive to compare the experimental data to these existing frameworks.

The strain invariant approach of Mooney–Rivlin, extensively used for filled rubbers, provides a straightforward approach for examining the deviation of a complex elastomeric system from ideality. The relationship between the stress (σ) and elongation ratio (λ) is expressed as

$$\sigma = 2\left(C_1 - \frac{C_2}{\lambda}\right)(\lambda - \lambda^{-2}) \quad (2)$$

where C_1 and C_2 are constants reflecting characteristics of the network. C_2 represents the non-Gaussian aspects of the network, such as physically (unstable) crosslinks. When $C_2 = 0$, $2C_1 = G$ (where G is the shear modulus) and Eq. (2) reduces to the well-known expression for the deformation of a Gaussian network.[25]

Figure 3 depicts the effective modulus [$\sigma/2(\lambda - \lambda^{-2})$] of the rubber/CNP composite with respect to the inverse elongation ratio (λ^{-1}). The affine deformation of an ideal Gaussian network ($C_2 = 0$) would appear as a horizontal line. The nanocomposites exhibited substantial nonideality during deformation, which was attributed to the metastability of physical crosslinks, complex morphology of hard-segment crystallites, and strain-induced crystallization of soft segments. This evolution of morphology was thought to be the primary source of hysteresis and cyclic softening. As the CNP loading increased, the nonideal behavior increased, especially at low deformation. After yield though ($\lambda \approx 1.81$), the relative behavior of the nanocomposites was similar, regardless of the CNP loading. Flandin et al.[29] observed similar results for the deformation of carbon-black-containing elastomers and rationalized a modulus scaling factor to superimpose curves based on a hydrodynamic perspective, where the effective modulus at any deformation depended only on the amount of filler. Following Flandin et al.,[29] Figure 4 emphasizes the similarity between all of the systems above yielding; this implies that the mechanistics of deformation beyond the yield point were dominated by the elastomer, with minimal impact from the CNPs. Also notable in Figure 5 is the appearance of a threshold volume fraction at which all nanocomposites behaved identically over the entire deformation range. Above ($V_c = 0.013$), the reduced Mooney–Rivlin curves deviated from this trend.

Influence of PE

Figure 5 depicts the stress–strain curves for rubber/CNP ($V_c = 0.013$) loaded with different concentrations of PE. From this figure, one can observe that at a fixed strain, the nanocomposite loaded with 12.4 vol % PE exhibited the highest stress and that

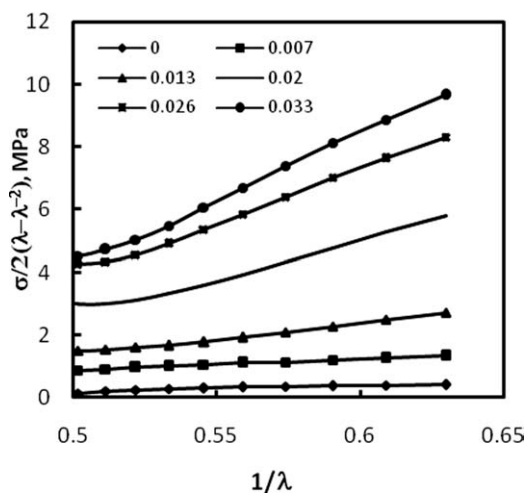

Figure 3 Effective modulus [$\sigma/2(\lambda - \lambda^{-2})$] of the rubber/CNP composite with respect to λ^{-1}.

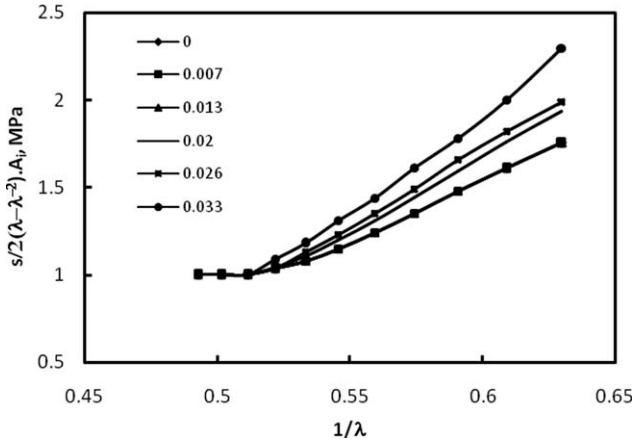

Figure 4 Reduced Mooney–Rivlin curves.

loaded with 3.2 vol % PE had the lowest stress. The energy absorbed per unit volume (W) in deforming the rubber composites to a strain (ε) was simply the area under the stress–strain curve and could be written as follows:

$$W = \oint \sigma(\varepsilon) d\varepsilon \tag{3}$$

where $\sigma(\varepsilon)$ is the stress as a function of the strain. Obviously, the higher the area under stress–strain curve is, the higher the energy absorption capacity is. As can be seen from Figure 5, among the rubber/PE/CNP composites, the composite loaded with 3.2 vol % PE had the lowest area under stress–strain curves and, thus, had the weakest absorption, whereas the composite loaded with 12.4 vol % PE had the strongest absorption. The energies absorbed by the rubber/CNP/PE (with concentrations of 3.2, 6.8, 12.4, and 17.1 vol %) composites were 24.6, 45.2, 61.5, and 32.1 MJ/m^3, respectively. On the other hand, the improvement in absorption efficiency should have made the impact protection more effective and more reliable.

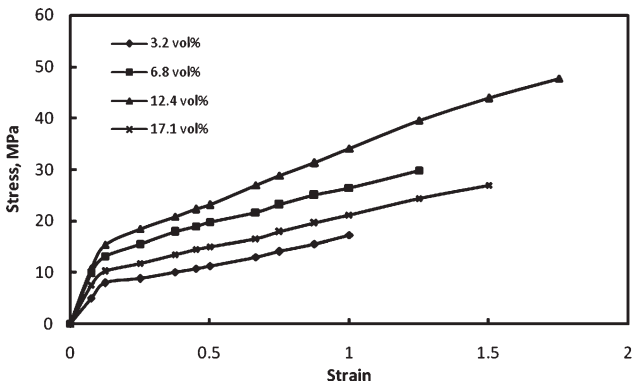

Figure 5 Stress–strain curves for rubber/(V_c = 0.013) CNP at different concentrations of PE.

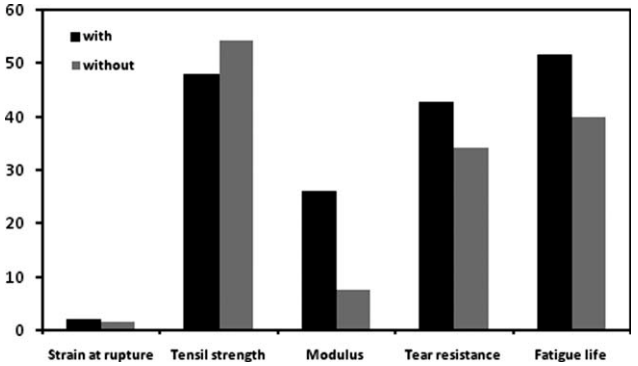

Figure 6 Mechanical parameters for the nanocomposites with and without PE.

Figure 6 depicts a comparison between rubber/(V_c = 0.013) CNP nanocomposites with and without PE (12.4 vol %) to indicate the effect of PE on the mechanical parameters. From Figure 7, one can notice that the addition of PE to the rubber/CNP composite decreased the tensile strength by 1.2% and increased the modulus by three times, whereas the strain at rupture was almost the same. From this figure, one can also notice that the addition of 12.4 vol % PE to the rubber/(V_c = 0.013) CNP nanocomposite increased the tear resistance by 12.1% and the fatigue life by 13.2%.

Morphology of nanocomposites

The morphology of the nanocomposites, and the degree of dispersion of nanofillers before and after cyclic fatigue in the rubber matrix were studied by scanning electron microscopy (SEM) and are shown in Figure 7. Considering the morphology of the fillers alone before cyclic fatigue, Figure 7(a) shows the SEM micrograph of the CNPs, which appeared to agglomerate in a spherical geometry, whereas the CNPs after addition of PE [Fig. 7(c)] did not show agglomeration to the same degree. The lack of any evidence of agglomeration, combined with the significant increase in the mechanical properties, indicated a good distribution of fillers in the rubber matrix as a result of the addition of PE; this increased the adhesion between the spherical CNPs and the rubber matrix.

Figure 7(b) shows the monotonic tensile fracture surface in the rubber containing CNPs after cycling fatigue. This figure shows a pullout of CNPs from the rubber matrix with a lot of large holes. Generally, there was a nonuniform distribution of the CNPs in the rubber and large, randomly distributed aggregates of carbon nanoparticles. These agglomerated regions were thought to be detrimental to strength and fatigue life. The distribution of CNPs into the rubber matrix after modification with PE

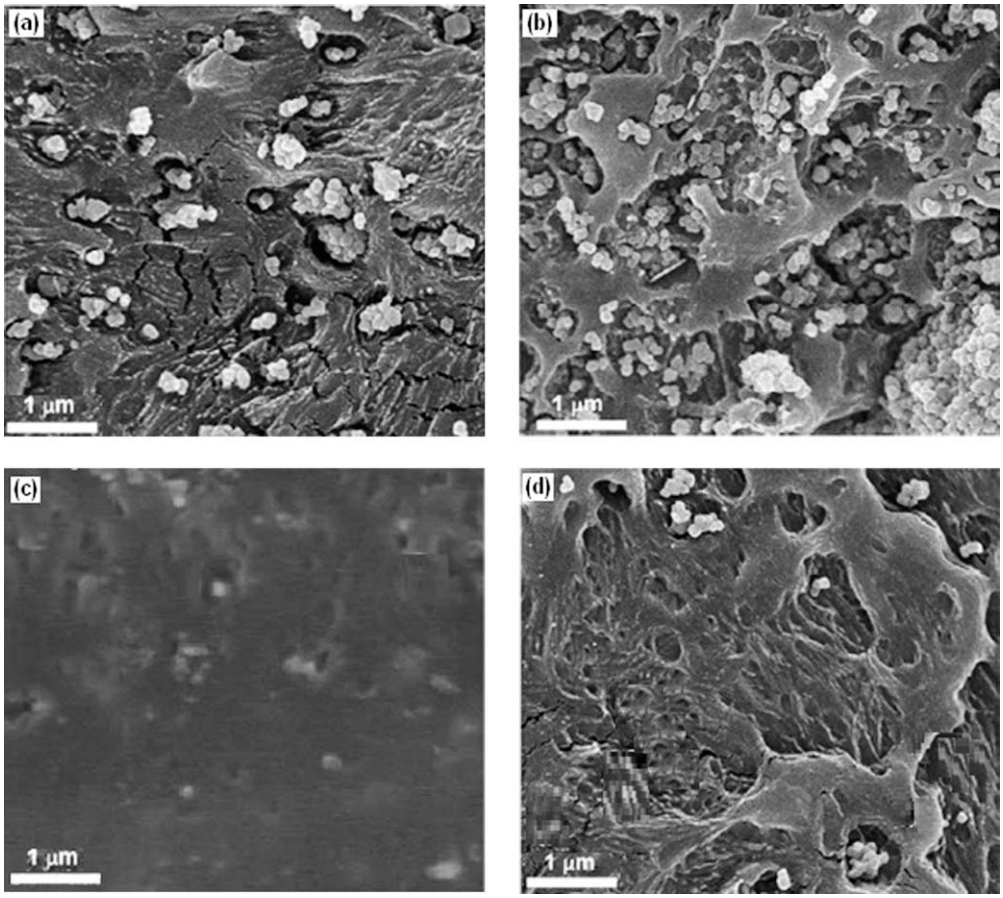

Figure 7 SEM photographs for NBR loaded with 1.3 vol % CNP (a) before (b) after cyclic fatigue and NBR loaded with 1.3 vol % of CNPs modified with PE (c) before and (d) after cyclic fatigue.

was better, and just very small aggregates appeared, pulled out from the nanocomposites. This indicates that the addition of PE enhanced the crosslinking between the CNPs and rubber matrix, which is believed to have contributed to the increased fracture resistance and significantly improved fatigue life.

Crosslink modeling

The effect of PE on the rubber/CNP composites can be discussed according to the crosslink model. The crosslink model describes the elasticity of a crosslink network by consideration of the additional contributions of finite chain extensibility to the elastic free energy (F):[25]

$$F = \frac{N_c kT}{2}\left[\left(\frac{\sum_i \lambda_i^2(1-\alpha^2)}{1-\alpha^2\sum_i \lambda_i^2}\right) + \log\left(1-\alpha^2\sum_i \lambda_i^2\right)\right] \quad (4)$$

where N_c is the crosslink density and α is a parameter describing the chain inextensibility. The summation is performed over three Cartesian components of strain (λ). For uniaxial tension, $\lambda_1 = \lambda$ and $\lambda_2 = \lambda_3 = \lambda^{-1/2}$. From the expression for stress

$$\sigma = \left(\frac{\partial F}{\partial \lambda}\right)_{T,V} \quad (5)$$

Equation (4) gives[30]

$$\sigma = N_c kT\left(\lambda - \frac{1}{\lambda^2}\right)\left[\frac{(1-\alpha^2)}{(1-\alpha^2\phi)} - \frac{\alpha^2}{(1-\alpha^2\phi)}\right] \quad (6)$$

where σ is the stress, λ is the extension ratio, k is the Boltzmann constant, T is the temperature, N_c is density of crosslinked chains with a functionality of four assumed, and ϕ is defined as

$$\phi = \lambda^2 + \frac{2}{\lambda} \quad (7)$$

Because the rubber modulus is defined as

$$G = \frac{\alpha}{\left(\lambda - \frac{1}{\lambda^2}\right)} \quad (8)$$

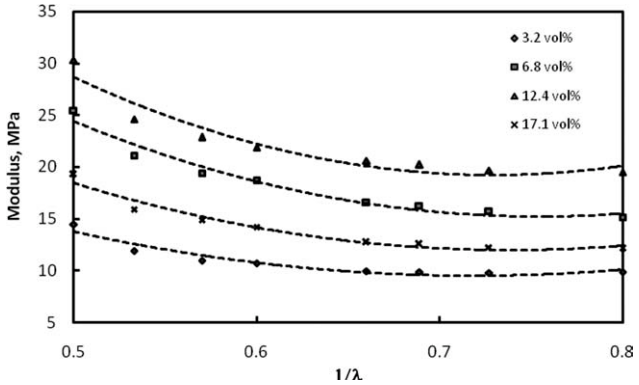

Figure 8 Variation of the modulus of elasticity with $1/\lambda$ at different concentrations of PE; the dot lines represent the data fitted with the crosslink model [Eq. (9)].

When one substitutes from Eq. (8) into Eq. (6), we get

$$G = N_c kT \left[\frac{(1-\alpha^2)}{(1-\alpha^2\phi)^2} - \frac{\alpha^2}{(1-\alpha^2\phi)} \right] \quad (9)$$

A two-parameter least-squares fit was performed to obtain α and N_c. The calculated modulus curves for the rubber/CNP/PE composites fit the entire range of deformation very well, as shown in Figure 8.

The fit parameters for the rubber nanocomposites are introduced in Table I. From such table, one can observe that the nanocomposites loaded with 12.4 vol % PE had an N_c at the optimum concentration of CNP. This meant that the PE enhanced the intercalation between CNPs with rubber at the percolation concentration of 12.4 vol %, where the hard domains acted as network junctions for the extensible soft segments.

The molecular weight of the chain segment between crosslinks (M_c) was obtained from N_c according to

$$M_c = \frac{\rho N_A}{N_c} \quad (10)$$

where ρ is the density and N_A is Avogadro's number. As expected, the nanocomposite at 12.4 vol % PE had a larger M_c than the other nanocomposites.

TABLE I
Crosslink Model Parameters

PE concentration (vol %)	α	N_c (10^{-26} m^{-3})	M_c (10^3 g/mol)
3.2	0.09 ± 0.01	1.21 ± 0.10	0.98 ± 0.10
6.8	0.24 ± 0.05	3.51 ± 0.24	1.42 ± 0.13
12.4	0.32 ± 0.03	6.72 ± 0.31	1.76 ± 0.11
17.1	0.17 ± 0.02	1.15 ± 0.11	1.28 ± 0.11

The values corresponded closely to the soft-segment molecular weight of the four nanocomposites. This supported the proposed structural model in which the hard domains acted as network junctions for the extensible soft segments. The somewhat low values of M_c compared to the soft-segment molecular weights was attributed to the multifunctionality of the hard-domain junctions and the high volume fraction of hard domains.

α was higher for 12.4 vol % PE than other PE concentrations. Inextensibility in the elastomers was attributed to finite chain length between immobile junctions,[25,30] although for 3.2 vol % PE, it was proposed that strain-induced crystallization accounted for the observed increase in the tensile stress.[31] In contrast, for 12.4 vol % PE, α described the constraint imposed by the partially continuous hard domains on the extension of the soft segments.

CONCLUSIONS

Different concentrations of CNPs were mixed with rubber. The results show that the CNPs improved the mechanical properties of this rubber by more than 15 times. The optimum concentration of investigated the rubber/CNP composites was found to be $V_c = 0.013$. The stress–strain relationship was fitted with the Mooney–Rivilin model. The results indicate that rubber/CNP followed an affine deformation mechanism. The influence of PE on the rubber/CNP composite caused increases in the tear resistance, modulus, and fatigue life and a decrease in the tensile strength, and the strain at rupture remained almost the same. The stress–strain relationship was fitted with the crosslink model. The results indicate that the addition of PE enhanced the intercalation between rubber and CNPs.

References

1. Long, Y.; Shanks, R. A. J Appl Polym Sci 1996, 61, 1877.
2. Bartczak, Z.; Argon, A. S.; Cohen, R. E.; Weinberg, M. Polymer 1999, 40, 2347.
3. Misra, R. K. D.; Nerikar, P.; Bertrand, K.; Murphy, D. Mater Sci Eng A 2004, 384, 284.
4. Unal, H.; Mimaroglu, A.; Alkan, M. Polym Int 2004, 53, 56.
5. Takahara, A.; Magome, T.; Kajiyama, T. J Polym Sci Part B: Polym Phys 1994, 32, 839.
6. Dibenedetto, A. T. Mater Sci Eng A 2001, 302, 74.
7. Sau, K. P.; Chaki, T. K.; Khastgir, D. Compos A 1998, 29, 363.
8. Ghosh, P.; Chakrabarti, A. Eur Polym J 2000, 36, 1040.
9. Job, A. E.; Oliveira, F. A.; Alves, N.; Giacometti, J. A.; Mattoso, L. H. C. Synth Met 2003, 135, 99.
10. Joly, S.; Gernaud, G.; Ollitrault, R.; Bokobza, L.; Mark, J. E. Chem Mater 2002, 14, 4202.
11. Potschke, P.; Bhattacharyya, A. R.; Janke, A. Polymer 2003, 44, 8061.
12. LeBaron, P. C.; Pinnavaia, T. J. Chem Mater 2001, 13, 3760.
13. Yu, M. F.; Lourie, O.; Dryer, M. J.; Molor, K.; Kelly, T. F.; Ruoff, R. S. Science 2000, 287, 637.

14. Yu, M. F.; Files, B. S.; Arepalli, S.; Ruoff, R. S. Phys Rev Lett 2000, 84, 5552.
15. Lux, F. J Mater Sci 1993, 28, 285.
16. Kirkpatrick, S. Rev Mod Phys 1973, 45, 574.
17. Zallen, R. The Physics of Amorphous Solids; Wiley: New York, 1985; Chapter 4.
18. Mahmoud, W. E.; El-Eraki, M. H. I.; El-Lawindy, A. M. Y.; Hassan, H. H. J Phys D 2006, 39, 2427.
19. Liu, Z. F.; Liu, Q.; Huang, Y.; Ma, Y. F.; Yin, S. G.; Zhang, X. Y.; Sun, W.; Chen, Y. S. Adv Mater 2008, 20, 3924.
20. Mahmoud, W. E.; El-Lawindy, A. M. Y.; El-Erak, M. H. I.; Hassan, H. H. J Sens Actuators A 2007, 136, 229.
21. El-Eraki, M. H. I.; El-Lawindy, A. M. Y.; Hassan, H. H.; Mahmoud, W. E. Appl Phys A 2007, 103, 2837.
22. Mahmoud, W. E.; Mansour, S. A.; Hafez, M.; Salam, M. A. J Polym Degrad Stab 2007, 92, 2011.
23. Mahmoud, W. E.; El-Eraki, M. H. I.; El-Lawindy, A. M. Y.; Hassan, H. H. J Phys D 2006, 39, 541.
24. El-Eraki, M. H. I.; El-Lawindy, A. M. Y.; Hassan, H. H.; Mahmoud, W. E. J Polym Degrad Stab 2006, 91, 1417.
25. Treloar, L. R. G. The Physics of Rubber Elasticity; Clarendon: Oxford, 1958.
26. Krigbaum W, R.; Roe, R.-J. Rubber Chem Technol 1965, 38, 1039.
27. Ferry, J. D. Viscoelastic Properties of Polymers, 3rd ed.; Wiley: New York, 1980; p 571.
28. Farago, O.; Kantor, Y. Europhys Lett 2000, 52, 413.
29. Flandin, L.; Chang, A.; Nazarenko, A.; Hiltner, E.; Baer, E. J Appl Polym Sci 2000, 76, 894.
30. Edwards, S. F.; Vilgis, T. Polymer 1986, 27, 483.
31. Ward, I. M.; Hadley, D. W. An Introduction to the Mechanical Properties of Solid Polymers; Wiley: New York, 1993; Chapter 3, p 41.